Materials Today Bio 30 (2025) 101382

Contents lists available at ScienceDirect

Materials Today Bio

journal homepage: www.journals.elsevier.com/materials-today-bio

A miR-activated hydrogel for the delivery of a pro-chondrogenic microRNA-221 inhibitor as a minimally invasive therapeutic approach for articular cartilage repair

Shan An [a,b], Claudio Intini [a,c], Donagh O'Shea [a,c], James E. Dixon [d,e], Yiran Zheng [b], Fergal J. O'Brien [a,c,f,*]

[a] Tissue Engineering Research Group (TERG), Department of Anatomy and Regenerative Medicine, RCSI, Dublin, Ireland
[b] College of Pharmaceutical Sciences, Soochow University, China
[c] Advanced Materials and Bioengineering Research Centre (AMBER), RCSI and TCD, Dublin, Ireland
[d] Regenerative Medicine & Cellular Therapies (RMCT), Biodiscovery Institute (BDI), School of Pharmacy, University of Nottingham, Nottingham, NG7 2RD, UK
[e] NIHR Nottingham Biomedical Research Centre, University of Nottingham, Nottingham, UK
[f] Trinity Centre for Biomedical Engineering, TCD, Ireland

ARTICLE INFO

Keywords:
Cartilage repair
miR-221 inhibitor
MeHA-Col I/Col II hydrogel
Gene therapy
Chondrogenesis

ABSTRACT

Articular cartilage has limited capacity for repair (or for regeneration) under pathological conditions, given its non-vascularized connective tissue structure and low cellular density. Our group has successfully developed an injectable hydrogel for cartilage repair, composed of collagen type I (Col I), collagen type II (Col II), and methacrylated-hyaluronic acid (MeHA), capable of supporting chondrogenic differentiation of mesenchymal stem cells (MSCs) towards articular cartilage-like phenotypes. Recent studies have demonstrated that silencing *miR-221* may be an effective approach in promoting improved MSC chondrogenesis. Thus, this study aimed to develop a *miR*-activated hydrogel capable of offering a more effective and less invasive therapeutic approach to articular cartilage repair by delivering a pro-chondrogenic *miR-221* inhibitor to MSCs using our MeHA-Col I/Col II hydrogel. The MeHA-Col I/Col II hydrogel was cast as previously shown and incorporated with cells transfected with *miR-221* inhibitor (using a non-viral peptide delivery vector) to produce the *miR*-activated hydrogel. Down-regulation of *miR-221* did not affect cell viability and enhanced MSCs-mediated chondrogenesis, as evidenced by significantly upregulated expression of key pro-chondrogenic articular cartilage genes (*COL2A1* and *ACAN*) without promoting hypertrophic events (*RUNX2* and *COL10A1*). Furthermore, *miR-221* down-regulation improved cartilage-like matrix formation in the MeHA-Col I/Col II hydrogel, with significantly higher levels of sulfated glycosaminoglycans (sGAG) and Col II produced by MSCs in the hydrogel. These results provide evidence of the potential of the *miR*-activated hydrogel as a minimally invasive therapeutic strategy for articular cartilage repair.

1. Introduction

Articular cartilage is a non-vascularized connective tissue with low cellular density, which under pathological conditions or damage has a limited capacity for repair, often leading to osteoarthritis (OA) [1]. OA is the most common chronic debilitating disease imposing a significant socioeconomic burden and affecting the quality of life of 500 million of people worldwide [2,3]. Pathologically, OA affects the whole joint including subchondral bone and soft tissues such as ligaments and the meniscus. OA triggers a series of deteriorative transformations within the extra-cellular matrix (ECM) of the articular cartilage. These changes involve modifications in ECM composition and structure, ultimately resulting in the substitution of healthy tissue with fibrous and calcified cartilage [4]. To date, the treatment of severe articular cartilage damage or disease can include pharmacological or surgical approaches. As pharmacological treatment, systemic drugs such as glucosamine sulfate and chondroitin sulfate has been used, in order to replenish cartilage components and have a nutritional effect on the tissue [5,6]. Moreover, the local intra-articular injections of hyaluronic acid (HA) can be an option in order to reduce friction between joints and reduce cartilage

* Corresponding author. Tissue Engineering Research Group (TERG), Department of Anatomy and Regenerative Medicine, RCSI, Dublin, Ireland.
E-mail address: fjobrien@rcsi.ie (F.J. O'Brien).

https://doi.org/10.1016/j.mtbio.2024.101382
Received 4 October 2024; Received in revised form 22 November 2024; Accepted 4 December 2024
Available online 5 December 2024

wear [7]. On the other hand, surgical treatments encompass methods such as bone marrow stimulation (BMS) techniques, autologous chondrocyte implantation (ACI), and cartilage graft-based repair (mosaicplasty) [4]. Although these approaches demonstrate partial effectiveness in addressing cartilage defect repair, their widespread utilization is hindered by their suboptimal long-term outcomes, which tend to deteriorate after a period exceeding five years, and often follow revision surgery for the patients [8,9]. Therefore, there is a significant clinical need for innovative solutions to repair articular cartilage and treat OA, as joint replacement often becomes the eventual outcome.

In this context, the field of tissue engineering and regenerative medicine (TERM) has emerged in the past two decades and shows some promise for treating articular cartilage defects and OA [10–15]. For instance, recent studies in our group have developed a type I/II collagen-hyaluronic acid (CI/II-HyA) porous scaffold capable of promoting the deposition of mature cartilage-like matrix while reducing hypertrophy and calcified cartilage formation [10,16]. In addition, we have recently begun to focus on developing alternative and minimally invasive therapeutic options for cartilage repair based on hydrogel biomaterials that can be used to treat defects through intra-articular injection. Hydrogels can offer advantages over prefabricated porous scaffolds in that may have higher biocompatibility with minimally invasive properties and can be used in the treatment of irregular-shaped defects [17,18]. For instance, they require smaller incisions and less disruption to muscles and tissues surrounding the knee, which leads to faster healing and less pain post-surgery [19]. The amphipathic nature of hydrogels enables them to mimic the high water content (up to 80 %) in the natural cartilage matrix [20,21]. To this end, a novel hydrogel, composed of collagen type I (Col I), collagen type II (Col II), and methacrylated-hyaluronic acid (MeHA), capable of supporting chondrogenic differentiation of mesenchymal stem cells (MSCs) towards articular cartilage-like phenotypes, as shown by the deposition of a sulfated glycosaminoglycans (sGAG) and collagen type II-rich matrix has been successfully developed in our group [22]. The inclusion of methacrylate groups enables photo-crosslinking, which imparts tunable mechanical properties to the hydrogel, making it more stable and resistant to degradation compared to traditional hyaluronic acid [23,24]. Building from this knowledge, in the present study, this MeHA-Col I/Col II hydrogel specifically designed for cartilage repair will serve as a delivery system for gene therapeutics, further enhancing its potential.

To achieve this, we propose the development of an advanced hydrogel capable of efficiently delivering therapeutic microRNA (miRNA) to MSCs in a controlled and sustained manner. MiRNAs are short, non-coding RNA molecules that regulate gene expression by targeting messenger RNAs to either inhibit their translation or promote their degradation [25–27]. Our group has demonstrated the capability of collagen-based biomaterials to deliver gene therapeutics such as plasmid-DNA (pDNA) and microRNA (miRNA) using non-viral vectors to enhance the repair of several tissues including cartilage, bone, skin and nerve [13,28–31]. Several studies show the capability of gene-activated scaffold-based platforms to enhance osteo/chondrogenesis [13,28–30]. For example, a gene-activated scaffold developed to deliver the *SOX Trio* (key cartilage transcriptional factor)-*S0X-5*, *SOX-6*, *SOX-9* has proved to improve chondrogenesis and the repair of cartilage in *vivo* [13]. In this study, *microRNA-221* (*miR-221*) was selected as a target of interest due to its role in the chondrogenic differentiation of MSCs [32–34]. Although the mechanisms through which *miR-221* interacts with cartilage-related transcriptional factors and various ECM components are complex and not fully elucidated, recent studies demonstrated that silencing *miR221* was highly effective in promoting improved chondrogenesis *in vitro* and enhanced cartilage repair *in vivo* [33–35]. Specifically, it has been hypothesized *miR-221* inhibitor treatment promotes chondrogenic processes since it leads to a weakening of the negative control that Snail Family Transcriptional Repressor 2 (*Slug*) exerts on chondrogenic factors and cartilage ECM proteins, such as collagen type II and aggrecan [33,34]. Therefore, this study aimed to further enhance the MeHA-Col I/Col II hydrogel for cartilage repair by delivering the therapeutic *miR-221* inhibitor in our hydrogel and assessing its chondrogenic potential in MSCs. We have exploited the GET system which has been shown to be effective in delivery several types of therapeutic genetic cargos such as pDNAs and miRNAs including peptides (Insulin and Oxytocin) [36–38].

Therefore, the main objective of this work was to develop an innovative *miR*-activated hydrogel for delivering a pro-chondrogenic *miR-221* inhibitor through a non-viral cell penetrating peptide based delivery system (GET) using the MeHA-Col I/Col II previously designed for cartilage repair (Fig. 1A). We hypothesized this *miR*-activated hydrogel would enhance MSC chondrogenesis and cartilage-like matrix deposition, offering a more effective and minimally invasive therapeutic approach to articular cartilage repair (Fig. 1B–C). To this end, the specific aims were: (1) to evaluate the capability of the *miR*-activated hydrogel in effectively down-regulating *miR-221* in MSCs while maintaining biocompatibility and avoiding cytotoxic effects, (2) to assess the hydrogel's ability to enhance MSC chondrogenesis and cartilage-like matrix formation, and (3) to evaluate the hydrogel's potential in promoting improved MSC chondrogenesis and the formation of high-quality hyaline-like cartilage without inducing hypertrophic events.

2. Materials and methods

2.1. Mesenchymal stem cell isolation and culture

Rat bone marrow-derived mesenchymal stem cells (MSCs) were isolated from 6 to 8 week old female Sprague Dawley rats (authorized by Research Ethics Committee of the Royal College of Surgeons in Ireland; application number REC202012003) using standardized protocols and including a stringent analysis of cell phenotype as previously described [39]. Bone marrow was harvested by flushing the femora of both hind limbs with growth media, which consisted of high-glucose Dulbecco's Modified Eagle Medium (DMEM) (Sigma-Aldrich, Ireland) supplemented with 20 % (v/v) fetal bovine serum (FBS) (ThermoFisher Scientific, Ireland), 0.002 % (v/v) primocin (ThermoFisher Scientific, Ireland), 1 % (v/v) GlutaMAX (ThermoFisher Scientific, Ireland), and 1 % (v/v) non-essential amino acids (ThermoFisher Scientific, Ireland). Cells were incubated under cell culture conditions (37 °C, 5 % CO_2 and 21 % O_2) for 24 h. Following incubation, the cell suspension was

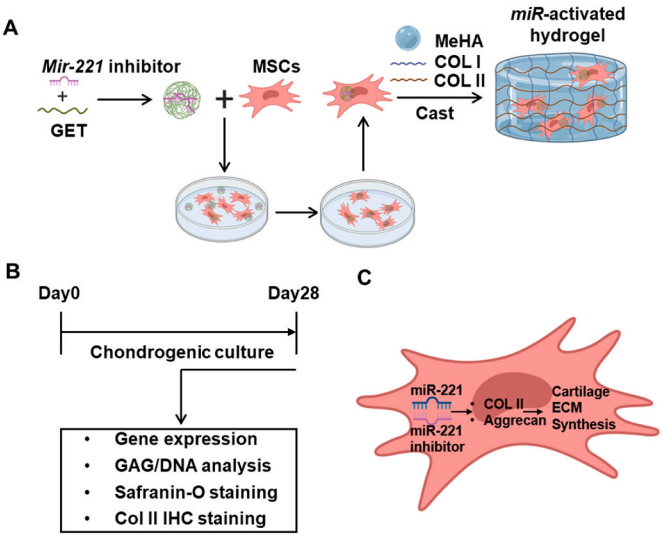

Fig. 1. Illustrative scheme describing the study design. (**A**) Illustrative scheme describing the experimental design. (**B**) Timeline of experiment conducted under chondrogenic condition. (**C**) The down-regulation of *miR-221* in mesenchymal stem cells significantly enhances chondrogenesis by upregulating key pro-chondrogenic genes and improving cartilage-like matrix formation.

centrifuged at 300×*g* for 5 min and resuspended in fresh growth medium under same conditions until passage 5 for experimental use.

2.2. Fabrication of collagen MeHA-Col I/Col II hydrogel

Methacrylated hyaluronic acid (MeHA) was synthesized using adapted protocols from our group [27]. Briefly, 1 % (w/v) solution of hyaluronic acid (HA) in dimethylformamide (DMF) was reacted with methacrylic anhydride (MA) at a 1:3 M ratio (HA disaccharide unit) while maintaining pH 8–9 with 5M NaOH. The mixture was stirred overnight at 2–8 °C. Sodium chloride was added to a final concentration of 0.5M, and MeHA was precipitated with ethanol. The product was purified by dialysis against deionized water for 5 days, lyophilized for 48 h, and stored at −20 °C. MeHA was dissolved in sterile PBS with 0.1 % Lithium phenyl-2,4,6-trimethylbenzoylphosphinate (LAP) photo-initiator to a concentration of 2 % (w/v) for use. Neutralized collagen type I (Col I; from bovine collagen, 35 mg/mL Lifeink 200®, Advanced BioMatrix) was purchased from (CellSystems Gmbh, Germany) and diluted to 2 % (w/v) using sterile PBS. Collagen type II (Col II; from porcine knee cartilage, Symatese, France) was dissolved in 0.5M acetic acid (Sigma Aldrich, Ireland) and subsequently neutralized using 5M NaOH to yield a final hydrogel concentration of 2 % (w/v). The hydrogel formulations were developed by mixing 2 % (w/v) MeHA with 1 % (w/v) Col I and 1 % (w/v) Col II in a 1:1 ratio.

2.3. Determination of methacrylated hyaluronic acid degree of functionalization

To assess the degree of HA functionalization with methacrylate groups, proton nuclear magnetic resonance (1H NMR) analysis was performed and averaged across three batches. The MeHA lyophilisate was dissolved to a concentration of 1 % (w/v) in deuterium oxide (D2O; Sigma Aldrich, Ireland), and 600 μL of this solution was transferred to a 5 mm diameter NMR tube (Sigma Aldrich, Ireland). The 1H NMR spectra were recorded on a Bruker Avance II 400 with UltraShield (Bruker GmbH, MA, USA). The data were analyzed using MestReNova software (version 6.0.2–5475, Mestrelab Research).

2.4. Transfection of MSCs with miR-221 inhibitor in 2D culture

To initially assess efficacy, cells were firstly transfected in 2-dimensional (2D) culture, a peptide-based non-viral vector, the GET (Glycosaminoglycan-binding Enhanced Transduction) peptide, was utilized as previously described [35]. MSCs at passage 4 were seeded at a density of $1x10^6$ cells per flask and cultured for 3 days in growth medium. Based on preliminary experimentation carried out in the laboratory, GET was used at a concentration of 1 mM and complexed to *miR-221* inhibitor (Horizon discovery, UK) prepared at a final concentration of 40 nM lfor 15 min in OptiMEM buffer (ThermoFisher Scientific, Ireland). GET--*miR-221* inhibitor complexes at a final volume of 50 μL were formulated at a charge ratio (CR) of GET to *miR-221* inhibitor CR 5:1, with the *miR-221* inhibitor concentration remaining constant at 40 nM. The medium was removed from each flask and replaced with 15 mL freshly complexed NP-containing medium. The flasks were then incubated at 37 °C for 1 day before the NP-containing medium was removed and replaced with fresh growth medium for a further 3 days.

2.5. Fabrication of cell-incorporated miR-activated MeHA-Col I/Col II hydrogels

MSCs were initially transfected with GET-*miR-221* inhibitor as previously described in Section 2.4, and then were trypsinized and re-suspended in 200 μL chondrogenic media (DMEM supplemented with 50 μg/mL ascorbic acid (Sigma-Aldrich, Ireland), 40 μg/mL proline (Sigma-Aldrich, Ireland), 100 nM dexamethasone (Sigma-Aldrich, Ireland), 1X ITS (BD Biosciences, UK), and 0.11 mg/mL sodium pyruvate (Sigma-Aldrich, Ireland)), such that 200 μL cell contained $2.5x10^6$ cells. To fabricate the *miR*-activated hydrogels, cell suspension was mixed with 1 mL of the MeHA-Col I/Col II hydrogel by passing the mixture between two coupled 5 mL syringes 30 times. *miR*-activated hydrogels were then injected into 6 mm × 5 mm Teflon molds and crosslinked under blue light at 405 nm for 2 min. The hydrogels were transferred into a 24-well suspension plate, and 1 mL of chondrogenic media was added to each well. Cell-free hydrogels were also manufactured as not treated (NT) group. The hydrogels were incubated at 37 °C with 5 % CO_2 for 28 days, with chondrogenic media changes three times a week.

2.6. Cellular metabolic activity assay

To determine the cellular metabolic activity and viability on the *miR*-activated hydrogels, an Alamar Blue assay was performed on the hydrogels. Metabolic activity of the MSCs in the hydrogel was assessed on day 1, 3, 7, 14, 21, and 28 using an AlamarBlue assay (Biosciences, Ireland) according to the manufacturer's instructions. Chondrogenic media containing 10 % (v/v) AlamarBlue solution was added at 37 °C for 2 h. A spectrophotometer (Wallac 1420 Victor2 D, USA) with an excitation wavelength of 550 nm and an emission wavelength of 590 nm was used to measure the resulting fluorescence levels. Chondrogenic media containing 10 % (v/v) AlamarBlue was used as a blank sample, and its fluorescence reading was subtracted from the experimental readings to eliminate background fluorescence.

2.7. Gene expression analysis

To determine the gene expression level of *miR-221* after transfecting the cells with the *miR-221* inhibitor, a quantitative real-time polymerase chain reaction (qRT-PCR) was conducted at day 3 (2D analysis) and day 21 (3D analysis). Total RNA was isolated using the *miRNeasy kit* (Qiagen, UK) and reverse transcribed to cDNA at a final concentration of 5 ng/μL using the TaqMan™ Advanced *miRNA* cDNA Synthesis Kit (ThermoFisher Scientific, Ireland). qRT-PCR was performed on a 7500 real-time PCR System (Applied Biosystems, UK) using the TaqMan™ Fast Advanced Master Mix (ThermoFisher Scientific, Ireland) with a validated TaqMan™ Advanced miRNA primer for hsa-*miR-221*-3p (ThermoFisher Scientific, Ireland). Additionally, total RNA previously isolated was reverse transcribed to cDNA at a final concentration of 2.5 ng/μL using the QuantiTect reverse-transcription kit (Qiagen, UK) and analyzed on the 7500 real-time PCR System. The relative expression of mRNA was calculated using the delta-delta Ct (ΔΔCt) method. The target mRNAs which are related to chondrogenic lineage were also measured: type II collagen alpha 1 chain (*COL2A1*), type I collagen alpha 1 chain (*COL1A1*), aggrecan (*ACAN*), Runt-related transcription factor 2 (*RUNX2*), type X collagen alpha 1 chain (*COL10A1*), and 18S ribosomal RNA (*18S*) served as the housekeeping gene (Table 1).

2.8. DNA quantification

To determine the DNA content per hydrogel, the Quant-iT™

Table 1
List of gene transcripts analyzed by qRT-PCR. Qiagen QuantiTect validated primers used to analyse the expression levels of target genes.

Target gene	Target gene reference	Catalogue code
Type II collagen alpha 1 chain (COL2A1)	Rn_Col2a1_1_SG	QT01084118
Type I collagen alpha 1 chain (COL1A2)	Rn_Col1a2_1_SG	QT01083467
Aggrecan (ACAN)	Rn_ACAN_1_SG	QT00189518
Runt-related transcription factor 2 (RUNX2)	Rn_RUNX2_1_SG	QT01300208
Type X collagen alpha 1 chain (COL10A1)	Rn_COL10a1_1_SG	QT00402479
18S ribosomal RNA (18S)	Rn_Rn18s_1_SG	QT02589300

PicoGreen® dsDNA assay kit (Invitrogen, UK) was used according to the manufacturer's instructions. The hydrogels were washed twice with PBS and subsequently digested in a papain enzyme solution at 60 °C for 12 h. This solution was prepared with 0.5M EDTA, cysteine-HCl, and 1 mg/mL papain enzyme (Carica papaya, Sigma-Aldrich, Ireland). DNA concentration was determined using a standard curve to estimate cell numbers. The DNA content in the hydrogels was measured on day 28.

2.9. Sulfated glycosaminoglycan (sGAG) quantification

To quantify the sulfated glycosaminoglycan (sGAG) content in the hydrogels, we utilized a Blyscan Sulfated Glycosaminoglycan Assay Kit (Biocolor Life Sciences, UK) following the manufacturer's instructions. Prior to digestion, as detailed in Section 2.8, the hydrogels were washed in PBS. The sGAG content was then determined using a standard curve and measured in the hydrogels on day 28.

2.10. Hematoxylin & eosin and Safranin-O histological staining

To determine the cellular and sGAG distribution, Hematoxylin & Eosin and Safranin-O histological staining were conducted within the MeHA-Col I/Col II hydrogels. The hydrogels were fixed in 30 % (w/v) sucrose for 4 h, followed by 15 % (w/v) sucrose overnight. They were then embedded in OCT medium and sectioned at various depths using a microtome (ThermoFisher Scientific, Ireland) to produce 7 μm thick slices. These sections were subsequently mounted on Polysine glass slides (Fisher-Scientific, Ireland) and the sections were hydrated in deionized water in preparation for staining. The sections were stained with Weigert's hematoxylin (Sigma Aldrich, Ireland) which stains nuclei black/dark purple, eosin (Sigma- Aldrich, Ireland), which stains the ECM pink, safranin-O (Sigma Aldrich, Ireland) which stains sGAG red, and fast green (Sigma Aldrich, Ireland) a light counterstain. Following, the sections were dehydrated and mounted with DPX (Sigma Aldrich, Ireland). Imaging was carried out using a Nikon Eclipse 90i microscope (Nikon Instruments Inc., NY, USA).

2.11. Collagen II immunohistochemical (IHC) staining

To detect Col II deposition in the hydrogels, immunohistochemical (IHC) staining was performed using established lab protocols [40]. Sections were blocked with IHC blocking buffer (1 % bovine serum albumin (BSA) and 5 % goat serum in PBS) and incubated overnight with anti-Collagen II antibody (1:1000, ab307674). The next day, sections were treated with HRP-conjugated secondary antibody (1:500, ab6728), followed by signal amplification using an avidin/biotin-based peroxidase system (PK-6101, Vector Laboratories, USA). DAB substrate peroxidase kit (SK-4100, Vector Laboratories, USA) was used for visualization. Slides were rinsed, dehydrated and mounted using DPX (Sigma Aldrich, Ireland). Imaging was done using a Nikon Eclipse 90i microscope (Nikon Instruments Inc., NY, USA).

2.12. Statistical analysis

Results are expressed as mean ± standard deviation unless otherwise stated. Statistical analysis was performed using GraphPad Prism software version 9.2.0 using a general linear model ANOVA with Fisher's LSD test analysis performed for multiple comparisons. p-values less than or equal to 0.05 ($p < 0.05$) were considered statistically significant. * denotes $p < 0.05$, ** = $p < 0.01$, *** = $p < 0.001$ and **** = $p < 0.0001$.

3. Results

3.1. 1H NMR analysis confirmed successful methacrylation of hyaluronic acid (HA)

1H NMR spectra were used to verify the methacrylation reaction and to determine the degree of functionalization of the HA backbone with methacrylate groups. 1H NMR analysis confirmed the successful methacrylation of hyaluronic acid (HA) by the appearance of a peak at approximately 1–2 ppm (peak 2) and two peaks at approximately 5–6 ppm (peak 3) in the MeHA spectrum (Fig. 2B). These peaks are absent in the HA spectrum, which only shows a characteristic peak at approximately 1–2 ppm (peak 1) revealing the alkyl group on the N-acetyl-D-glucosamine subunit (Fig. 2A).

3.2. miR-221 is successfully down-regulated in MSCs in 2D and hydrogel

To evaluate delivery efficiency, the capability of GET to deliver the *miR-221* inhibitor to MSCs in a 2D culture model was initially investigated. The results demonstrated that the delivery of the GET-*miR-221* inhibitor to MSCs significantly reduced *miR-221* expression by day 3 ($p < 0.01$) compared to the non-treated (NT) group (Fig. 3A). Specifically, *miR-221* expression in the inhibitor-treated group was reduced by 91 %, highlighting the effective transfection and delivery of the *miR-221* inhibitor mediated by the GET peptide delivery vector.

After confirming that *miR-221* can be successfully down-regulated in MSCs in a 2D culture system, the capability of GET to deliver the *miR-221* inhibitor to MSCs in our 3D *miR*-activated hydrogel was investigated by analyzing *miR-221* expression via qPCR on day 21. Results showed that in each biological repeat, the expression of *miR-221* significantly decreased on day 21 in the *miR-221* inhibitor group. Overall, it revealed that *miR-221* expression levels in *miR*-activated hydrogels were significantly reduced by 75 % compared to NT group ($p < 0.05$) (Fig. 3B). This indicates that the *miR*-activated hydrogel can down-regulate *miR-221* expression in MSCs in a stable and controlled manner up to day 21.

3.3. miR-221 down-regulation did not affect MSC viability in miR-activated hydrogels

To assess biocompatibility, the impact of *miR-221* down-regulation on the viability of MSCs in the hydrogels was evaluated. Results overall revealed that *miR-221* down-regulation did not negatively affect cell viability in *miR*-activated hydrogels compared to *miR*-free hydrogels (Fig. 4). Specifically, there was no significant difference in cell metabolic activity and DNA content between the *miR*-activated hydrogel group and the NT group transitioning from day 1 to day 28 (Fig. 4A–B). The *miR*-activated hydrogel group had a DNA content of 240.0 ± 61.74 ng/mL at day 28, while the NT group had 249.4 ± 159.8 ng/mL, showing no significant difference between the two groups (Fig. 4B). This indicates that the reduction in *miR-221* expression does not affect the viability of MSCs grown on MeHA-Col I/Col II hydrogels.

3.4. miR-activated hydrogels enhanced MSC chondrogenesis by upregulating key chondrogenic genes and without prompting hypertrophic genes

Further analysis of the effect of *miR-221* down-regulation on MSC chondrogenic differentiation was then investigated by measuring the expression of specific genetic markers typically associated with effective MSC chondrogenesis and late-stage differentiation. The down-regulation of *miR-221* in *miR*-activated hydrogels overall enhanced MSC chondrogenesis with up-regulation of key pro-chondrogenic genes at day 21 (Fig. 5). Specifically, *miR*-activated hydrogels significantly upregulated *COL2A1* ($p < 0.01$), *ACAN* ($p < 0.05$) expression and *COL2A1/COL1A2* ($p < 0.01$). The *COL2A1/COL1A2* ratio serves as an important indicator of cartilage differentiation, with a higher ratio reflecting greater chondrogenic maturation and cartilage-specific matrix production by day 21, compared to NT samples (Fig. 5A–C). Despite the lack of significant difference between the *miR-221* inhibitor group and the NT group in the biological repeat 3, overall, the *miR-221* inhibitor group exhibited a 33-fold increase in *COL2A1* expression, a 7-fold

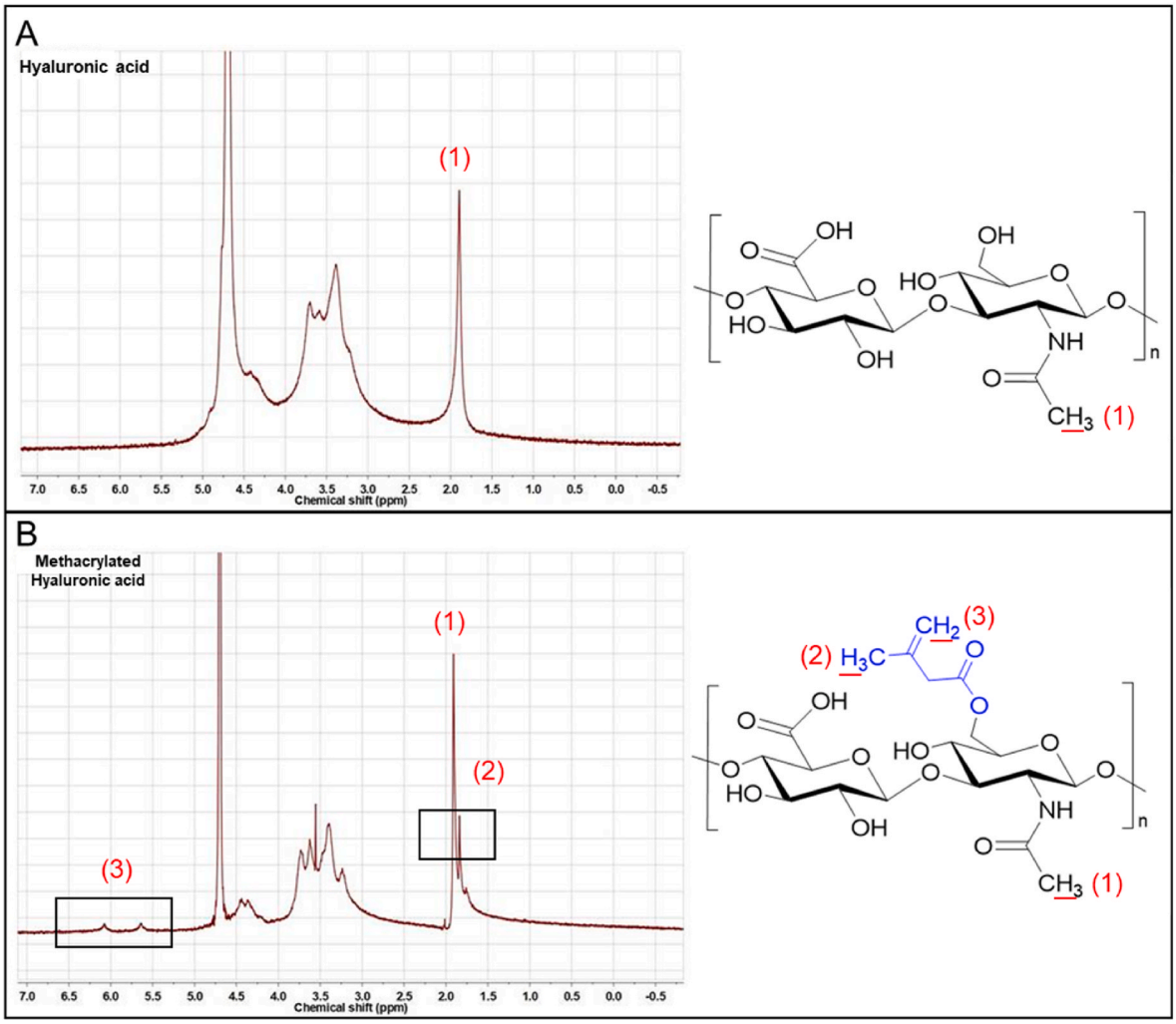

Fig. 2. 1H-NMR characterisation of methacrylated hyaluronic acid (MeHA) indicates the incorporation of methacrylate groups onto the HA backbone. The presence of **(B)** a peak at approximately 1–2 ppm (2) and two peaks at approximately 5–6 ppm (3) in the MeHA 1H NMR spectrum, which are absent in the **(A)** HA 1H NMR spectrum, indicate the presence of methacrylate groups on the HA backbone.

increase in *ACAN* expression, and a 34-fold increase in the *COL2A1/COL1A2* ratio compared to the NT group. These findings indicate that *miR*-activated hydrogels enhance MSC chondrogenesis. Additionally, and importantly, *miR*-activated hydrogels did not affect the expression of *COL1A2*, *RUNX2* and *COL10A1* - genes associated with MSC hypertrophy, a key problem in therapeutic cartilage repair that often leads to the formation of lower-quality cartilage tissue, unable to meet the necessary mechanical and biological functions required for effective repair (Fig. 5D–F).

3.5. *miR-221 down-regulation in miR-activated hydrogels increased MSC-mediated sGAG synthesis by day 28*

Further analysis of the effect of *miR-221* down-regulation on cartilage-like matrix formation *in vitro* was conducted in the *miR*-activated hydrogels. The results demonstrated that the *miR*-activated hydrogels enhanced sulfated glycosaminoglycan (sGAG) production compared to NT group (Fig. 6). Specifically, we observed that *miR-221* down-regulation led to a significant increase in sGAG deposition in biological repeats 1 and 3. However, this effect was not evident in biological repeat 2. In general, *miR-221* inhibitor group exhibited significantly higher ($p < 0.05$) levels of sGAG, with a value of 55.21 ± 49.59 (μg/ml), which was approximately three times higher compared to the NT group (19.59 ± 8.64 μg/mL) (Fig. 6A). When sGAG levels were normalised to DNA content, the same notable increase in sGAG/DNA with the down-regulation in *miR-221* expression can be observed in both biological repeat 1 and biological repeat 3. However, no obvious difference was observed in biological repeat 2. The *miR-221* inhibitor group had a sGAG/DNA ratio of 202.3 ± 147.1(μg/μg), it was approximately three times greater which was also significantly higher ($p < 0.05$) than the NT group with a value of 96.24 ± 63.61(μg/μg) (Fig. 6B).

3.6. *All hydrogels promoted a homogeneous cartilage-like distribution, with the miR-activated hydrogels showing a more abundant sGAG deposition*

To qualitatively assess the impact of *miR-221* down-regulation on MSC migration and matrix formation/distribution, hematoxylin & eosin and safranin-O staining were performed on the *miR*-activated hydrogels. Histology results revealed a homogenous cellular distribution throughout the hydrogels in all groups with a greater sGAG distribution in *miR*-activetd hydrogels (Figs. 7–8). Specifically, *miR-221* down-regulation in *miR*-activated hydrogels revealed a more abundant sGAG deposition in biological repeats 1 and 3 compared to the NT group. However, in biological repeat 2, no significant increase in sGAG distribution was observed in the *miR-221* inhibitor group compared to the NT group, which aligns with the sGAG quantitative analysis results (Fig. 8).

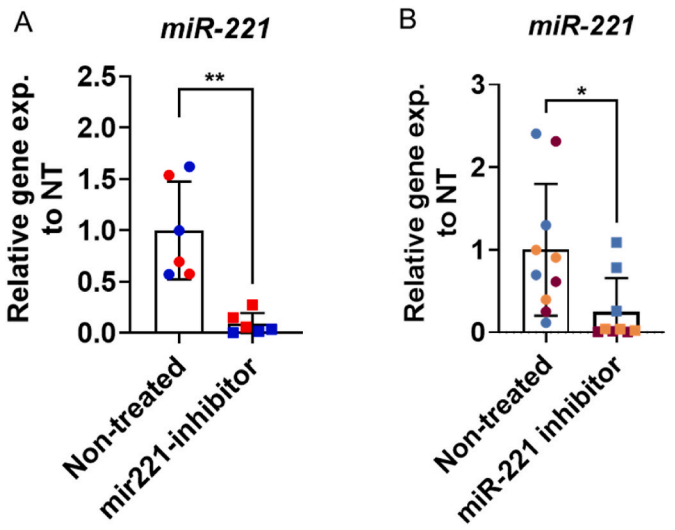

Fig. 3. Down-regulation of *miR-221* in MSCs in 2D culture and hydrogel. **(A)** *miR-221* is successfully down-regulated in MSCs in 2D at day 3. **(B)** *miR-221* is down-regulated in MSCs using miR-activated hydrogels up to day 21. Expression of *miR-221* was determined after 3 days in 2D and 21 days in hydrogel, normalised to *18S* and then converted to a fold increase in expression using the formula: Fold increase = 2-(ΔΔCt). Red represents biological repeat 1, blue represents biological repeat 2 in Fig. 3A, data shown represents from two individual MSC biological repeats (n = 2 per biological repeat) ± SD. **denotes $p < 0.01$; Red represents biological repeat 1, blue represents biological repeat 2, and orange represents biological repeat 3 in Fig. 3B, data shown represents from three individual MSC biological repeats (n = 3 per biological repeat) ± SD. * denotes $p < 0.05$.

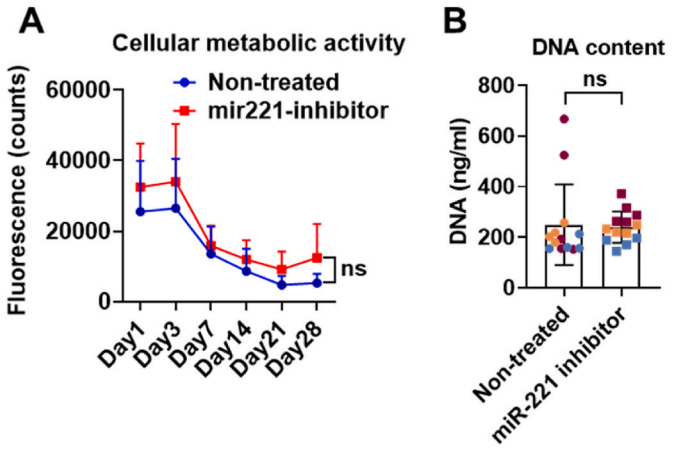

Fig. 4. The down-regulation of *miR-221* had no impact on MSC viability and proliferation. (**A**) Cellular metabolic activity per hydrogel was determined at day 1, 3, 7, 14,21 day and 28 days in chondrogenic culture. (**B**) DNA content per hydrogel was determined after 28 days in chondrogenic culture. Red represents biological repeat 1, blue represents biological repeat 2, and orange represents biological repeat 3. Data shown represents from three individual MSC biological repeats (n = 3 per biological repeat).

3.7. miR-activated hydrogels enhanced MSC chondrogenesis by upregulating key chondrogenic genes and without prompting hypertrophic ones

To qualitatively assess the cartilage-like matrix formed in the *miR*-activated hydrogels, collagen type II (Col II) (a main articular cartilage component) IHC staining was performed following 28 days culture. IHC revealed that *miR*-activated hydrogels overall sustained higher-quality cartilage-like matrix formation compared to NT group (Fig. 9). Specifically, results display much higher level of Col II MSC-mediated synthesis in the *miR*-activated hydrogels in biological repeat 1 and 2 compared to NT group. This indicates that *miR-221* down-regulation in *miR*-activated hydrogels promotes the synthesis of a high-quality cartilage-like matrix. However, in biological repeat 3, there is no obvious difference in Col II synthesis between the *miR-221* group and the NT group. Interestingly, this aligns with the PCR results on day 21 (Fig. 5) — *COL2A1* expression is significantly increased with *miR-221* down-regulation in biological repeats 1 and 2, but not in biological repeat 3.

4. Discussion

The main goal of this study was to develop an innovative *miR*-activated hydrogel through the delivery of a pro-chondrogenic *miR-221* inhibitor to enhance MSC chondrogenesis and cartilage-like matrix formation for a more effective and minimally invasive therapeutic approach to articular cartilage repair. To achieve this, a MeHA-Col I/Col II hydrogel previously developed in our group for cartilage repair was used as a platform for therapeutic delivery of an inhibitor to *miR-221* which has been shown to enhance MSC chondrogenesis and the formation of cartilage-like tissue in both *in vitro* and *in vivo* models [33,41]. The *miR*-activated hydrogel demonstrated successful, controlled, and sustained down-regulation of *miR-221* for up to 21 days. The down-regulation of *miR-221* enhanced MCS chondrogenesis by upregulating key pro-chondrogenic articular cartilage genes (*COL2A1* and *ACAN*), without inducing hypertrophic markers such as *RUNX2* and *COL10A*. In addition, *miR-221* down-regulation also led to improved cartilage-like matrix formation evidenced by increased deposition and distribution of sGAG and *Col II* (key components of healthy articular cartilage). Taken together, this study presents, for the first time, a novel *miR*-activated hydrogel capable of significantly enhancing MSC chondrogenesis and promoting high-quality/quantity cartilage-like formation, demonstrating strong potential as a minimally invasive therapeutic alternative to current clinical treatments for articular cartilage repair.

Biologically, the newly developed injectable *miR*-activated MeHA-Col I/Col II hydrogel exhibited excellent biocompatibility, with no cytotoxic effects on MSCs observed up to day 28. These findings are not surprising and consistent with our previous studies, which showed that the previously developed hydrogel used in this study well supports cell viability after injection or 3D printing [22]. These findings also align with studies from other researchers demonstrating the biocompatibility of hyaluronic acid (HA)-based natural biopolymers [41–43]. For instance, Insup et al. demonstrated that an HA, hydroxyethyl acrylate (HEA), and gelatin-methacryloyl (HA-g-pHEA-gelatin) gel exhibited excellent biocompatibility, with bone cells loaded into the hydrogel remaining viable, proliferating well, and spreading effectively [43]. Another study reported that a polylactic acid (PLA)-HA-based hydrogel maintained high cell viability over a long-term culture period of up to four weeks, preserving human chondrocyte morphology throughout [42]. Similarly, Lolli et al. found that a fibrin/HA hydrogel provided a supportive environment for cell transfection while maintaining high viability for up to 14 days in culture [41]. These results suggest that the *miR*-activated hydrogel developed in this study is not only effective but also a safe and versatile biomaterial. Its biocompatibility and structural properties make it promising for cartilage repair through the delivery of therapeutic miRNAs. This supports its potential for use in regenerative medicine and minimally invasive therapies aimed at tissue repair and regeneration.

Furthermore, the *miR-221* activated hydrogel demonstrated success in effectively down-regulate MSCs-mediated *miR-221* gene expression in a sustained and controlled manner up to 21 days *in vitro*, demonstrating the efficacy of the employed non-viral delivery system (GET peptide). This results are comparable to what was shown previously in our lab revealing the successful down-regulation of *miR-221* in human-derived MSCs up to day 28 when using a porous lyophilized scaffold platform [35]. However, while GET delivery system has shown to transfect

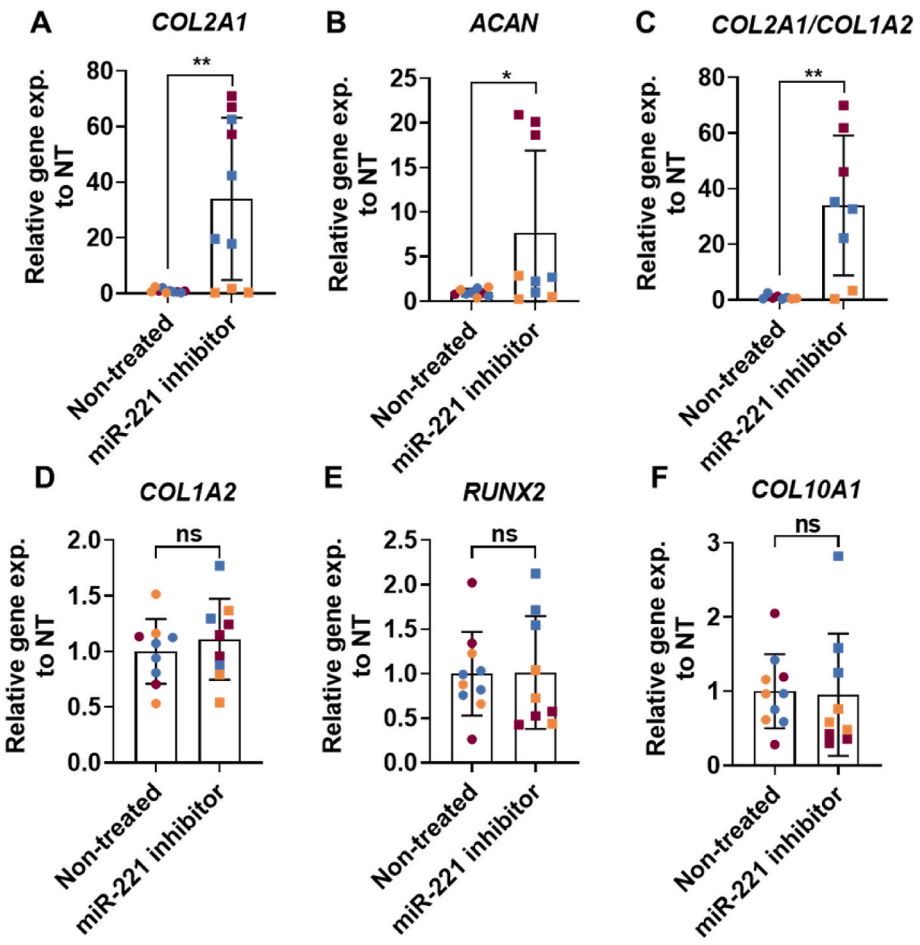

Fig. 5. The down-regulation of *miR-221* in *miR*-activated hydrogels enhanced MSC chondrogenic differentiation. The gene expression of (**A**) *COL2A1*; (**B**) *ACAN*; (**C**) *COL2A1/COL1A2*; (**D**) *COL1A2;* (**E**) *RUNX2* and (**F**) *COL10A1* was determined after 21 days, normalised to *18S*, then converted to fold increase in expression using the formula: Fold increase = 2-(ΔΔCt). Red represents biological repeat 1, blue represents biological repeat 2, and orange represents biological repeat 3. Data shown represents from three individual MSC biological repeats (n = 3 per biological repeat) ± SD. * denotes $p < 0.05$, ** = $p < 0.01$.

genetic cargos such as plasmid DNAs (pDNAs), modified messenger RNAs (mRNAs) and microRNAs (miRNAs) to several different cell types with high efficiency, and with no impact on cellular cytotoxicity, our study shows, for the first time, its ability to effectively and safely deliver a therapeutic miRNA through a gene-activated hydrogel [13,35]. While traditional porous scaffold biomaterials used for joint cartilage repair typically require an invasive surgical intervention, our study offers a novel approach for minimally invasive delivery of *miR-221* inhibitor to stimulate endogenous cartilage repair based on its potential as injectable delivery system [44]. Minimally invasive surgical procedures for knee issues offer several benefits compared to traditional surgery [45]. For instance, they require smaller incisions and less disruption to muscles and tissues surrounding the knee, which leads to faster healing and less pain post-surgery as well as a reduced operating time and lower risk of infection or other surgical complications [19]. Our approach offers faster recovery times due to its less invasive nature and its design to mimic natural articular cartilage tissue [46]. For clinical applications, MSCs will first be isolated from the patients and transfected in 2D culture, and then encapsulated in the hydrogel. Afterward, the miR-activated hydrogel will be injected into the joint cavity and cross-linked by UV light. As a result, patients can experience quicker recoveries, allowing them to return to daily activities or physical therapy sooner. Additionally, the process of making hydrogel is straightforward, eliminating the need for more complex scaffolds preparation methods such as melt molding, 3D printing or freeze-drying. In addition, this innovative *miR*-activated hydrogel platform is sufficiently adaptable to be utilized in many other tissue engineering applications such as skin and bone or even potentially cardiac and nervous system applications.

As downstream result of *miR-221* down-regulation, the *miR*-activated hydrogel proved to support a robust and enhanced MSC chondrogenesis, leading to a significant increase in sGAG and collagen type II (Col II) deposition. These findings align with previous studies from other groups and our laboratory showing a significant benefit on MSC chondrogenesis when *miR-221* intracellular pathway is disrupted [33,35,41]. For instance, the intracellular silencing of *miR-221* in MSCs cultivated in 3D pellet systems up to 21 days prompt a beneficial chondrogenic effect with improved sGAG and Col II deposition *in vitro* [41]. Similarly, the silencing of *miR-221* increased human-derived MSC-mediated sGAG normalised to DNA synthesis at day 28 when seeded in a highly porous biomaterial scaffold [35]. However, although *miR-221* down-regulation shown some promise with improved overall sGAG deposition in porous biomaterial scaffolds (not significant), in our study the *miR*-activated hydrogel showed significantly higher (3-fold) levels of sGAG by day 28 when compared to *miR*-free samples [35]. These findings suggest an improved therapeutic effect for the *miR*-activated hydrogel on cartilage-like matrix formation over traditional scaffolds. Traditional scaffolds often use a cell seeding method that may result in cell loss, while the *miR*-activated hydrogel allows for direct cell incorporation with higher-density and uniform cell encapsulation. This approach can improve intercellular connections and cell–cell contacts, thus playing a crucial role in enhancing MSC chondrogenic differentiation as shown by numerous studies [33,47,48]. Therefore, the observed increase in sGAG

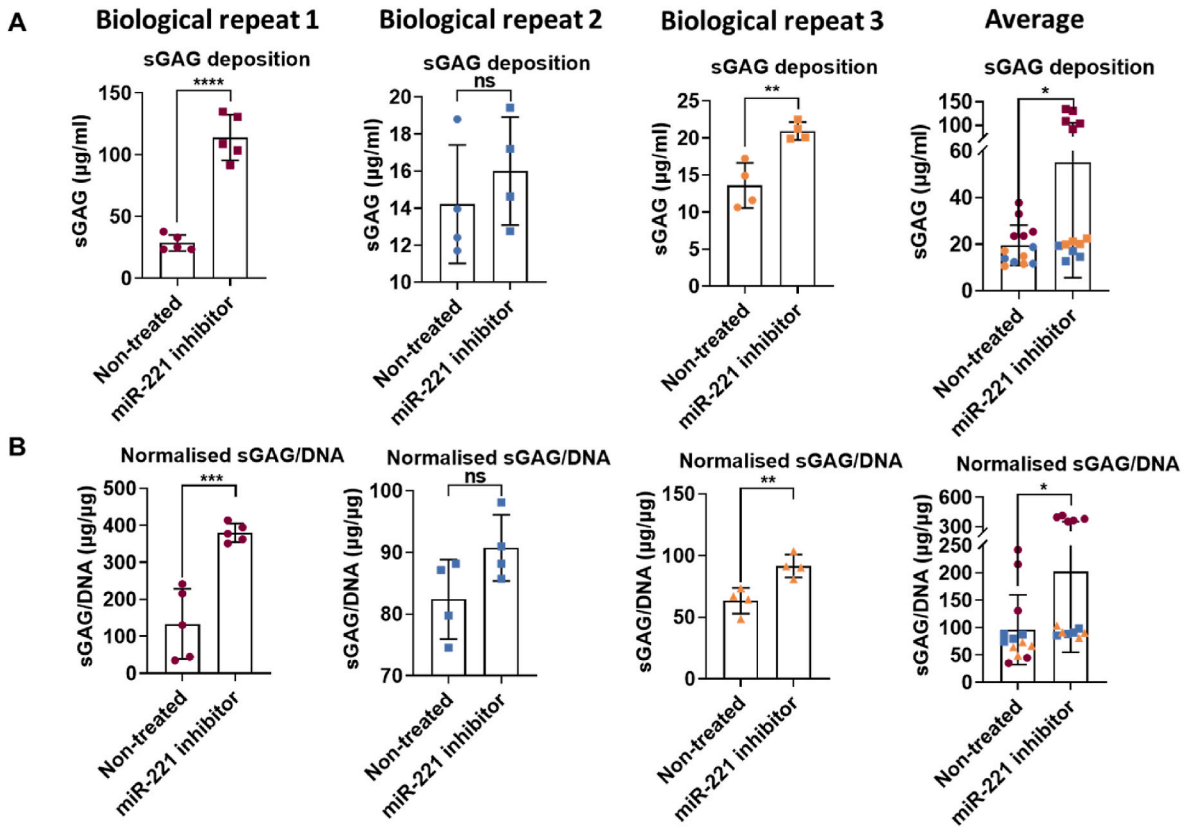

Fig. 6. ***miR*-activated hydrogels increased MSC-mediated sGAG synthesis at day 28.** (**A**) Overall sGAG per hydrogel (**B**) and sGAG normalised to DNA content respectively were determined after 28 days in chondrogenic culture. The data represent three individual MSC biological replicates (red: biological repeat 1; blue: biological repeat 2; orange: biological repeat 3) along with the mean value across all three replicates (n = 3 per biological repeat).

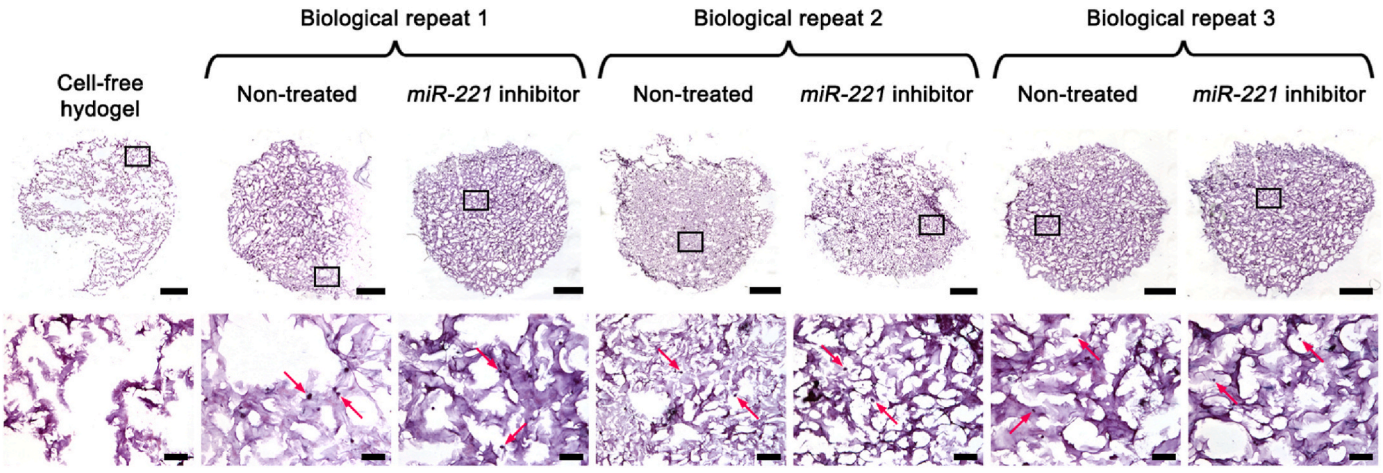

Fig. 7. All hydrogels sustained a homogenous cellular distribution. MSCs distribution in hydrogel following 28 days chondrogenic culture, as shown by biological repeat 1, 2 and 3 Hematoxylin & Eosin staining. Cell nuclei are stained in blue and ECM in pink (Scale bar for first row images represents 1 mm and for second row 100 µm; the second row shows enlarged versions of the images in the first row, with markers indicating their corresponding positions). Staining was also performed on cell-free hydrogels.

production is likely attributable to the improved cell-cell interactions provided by the 3D culture environment within the hydrogel.

Furthermore, gene expression analysis revealed a significant up-regulation of *COL2A1*, *ACAN* and the *COL2A1/COL1A2* ratio (typical key pro-chondrogenic genes associated to successful MSC chondrogenesis) when *miR-221* was down-regulated in the miR-activated hydrogel. This aligns with findings from previous research where intracellular silencing of *miR-221* in MSCs in 3D pellet systems led to increased *COL2A1* and *ACAN* expression at day 21[41]. However, while our results were aligned with findings in 3D pellet systems, they were in contrast with prior experiments from our group which did not show upregulation of *ACAN* and *COL2A1* when *miR-221* was down-regulated in a porous biomaterial scaffold [49]. As previously mentioned, this difference likely stems from the improved cell-cell interactions and uniform cell distribution achieved in the cell-incorporated hydrogel [33,47,48]. As a result, the *miR*-activated hydrogel demonstrates the

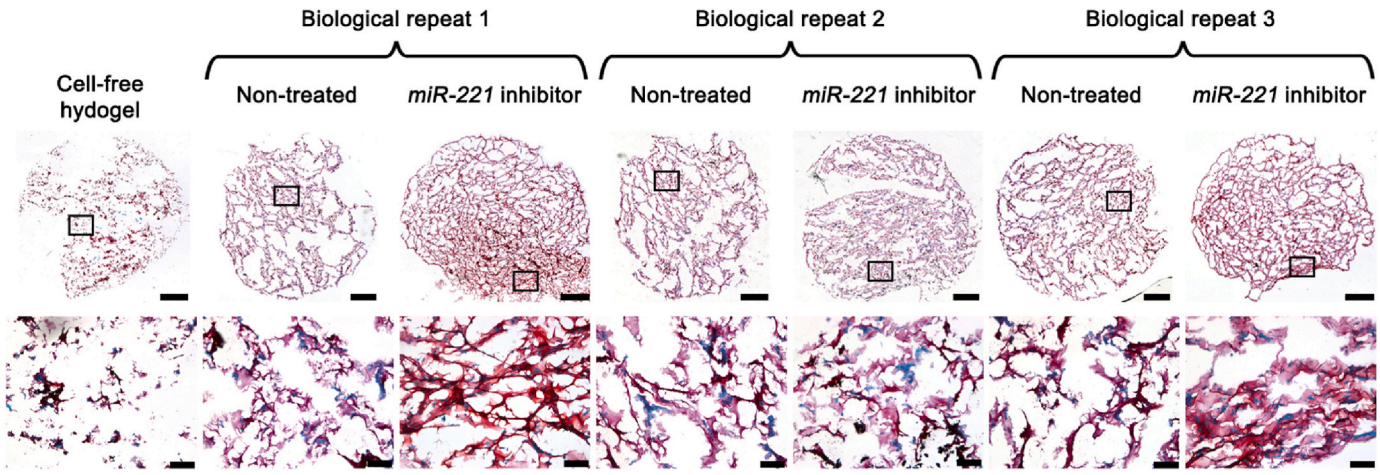

Fig. 8. *miR*-activated hydrogels promoted a more abundant and homogenous sGAG deposition. sGAG deposition by MSCs in hydrogel following 28 days chondrogenic culture, as shown by biological repeat 1, 2 and 3 Safranin-O staining. sGAGs are stained in red (Scale bar for first row images represents 1 mm and for second row 100 μm; the second row shows enlarged versions of the images in the first row, with markers indicating their corresponding positions). sGAG presence was also assessed on cell-free hydrogels.

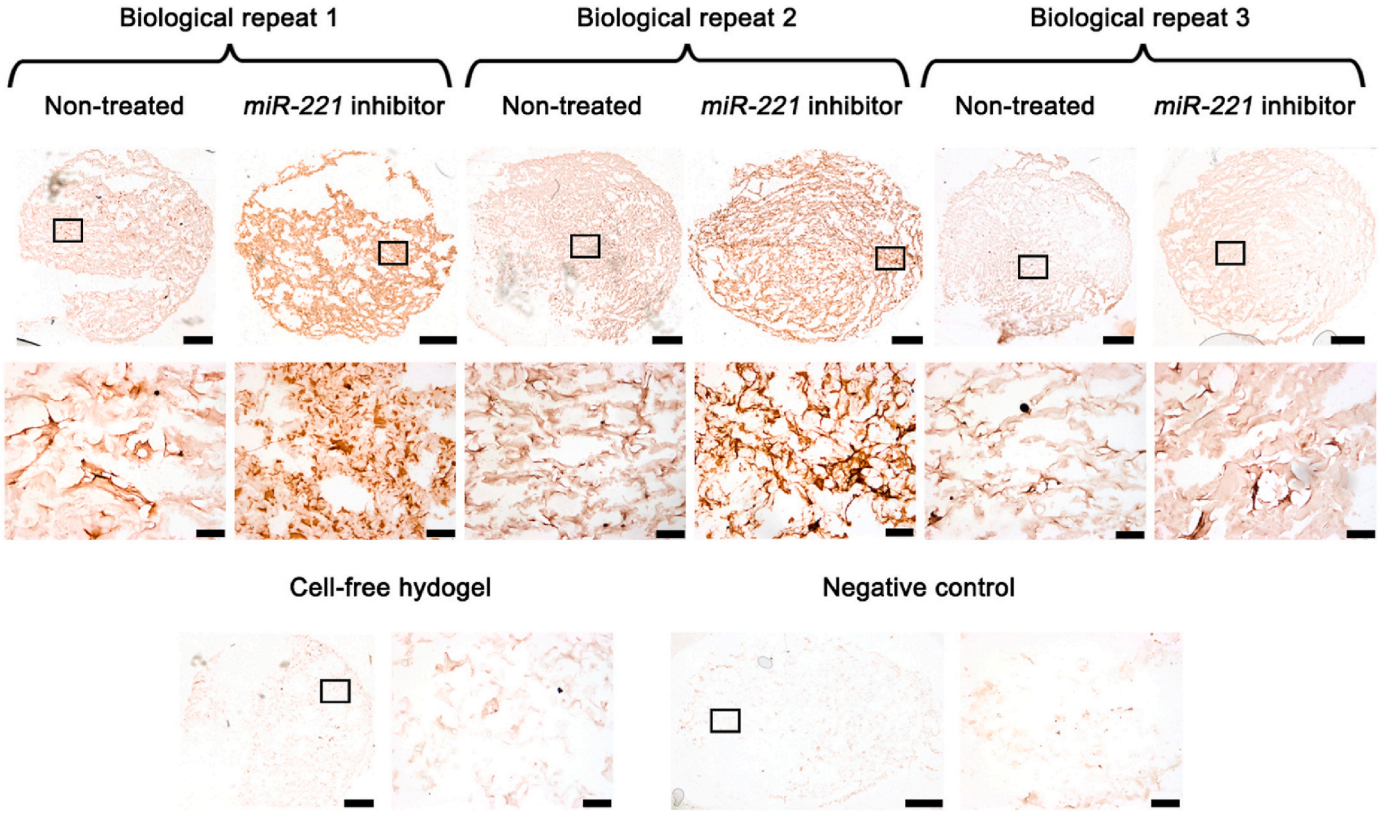

Fig. 9. *miR*-activated hydrogels promoted the synthesis of high-quality cartilage-like matrix. Col II deposition by MSCs in hydrogel following 28 days chondrogenic culture, as shown by biological repeat 1, 2 and 3 Col II IHC staining. Col II is stained brown (scale bar from first row images represents 1 mm and for second row 100 μm; the second row shows enlarged versions of the images in the first row, with markers indicating their corresponding positions). Coll II was also assessed on cell-free hydrogels. Negative control (hydrogel without Coll II primary antibody) was included, as shown in the third row of the image.

potential to produce higher-quality cartilage and to enhance chondrogenesis, offering a more durable solution for cartilage repair in clinical applications. Moreover, while *miR-221* down-regulation in *miR*--activated hydrogel enhanced chondrogenesis and *de novo* engineered cartilage, it did not induce up-regulation of hypertrophic markers (*RUNX2* and *COL10A1*), which often leads to hypertrophic cartilage and mechanically unfunctional tissue. Although previous research has demonstrated that *miR-221* down-regulation can reduce hypertrophic events by significantly lowering *RUNX2* expression at both the gene and protein levels by day 28, this was not seen in our study. Therefore, these findings highlight the need for further research to elucidate the intracellular mechanisms of miR-221 during MSC chondrogenic differentiation, particularly its interactions with cartilage-related transcriptional factors and various extracellular matrix (ECM) components. While additional studies are essential to clarify these pathways, our findings provide a foundation for future investigations into the role of miR-221 in

regulating MSC chondrogenic differentiation, with a specific focus on its contribution to maintaining the balance between chondrogenic and hypertrophic differentiation.

Overall, the study not only shows the biocompatibility of MeHA-Col I/Col II hydrogel for cell culture but also indicates its potential as a *miR*-activated hydrogel for directing more effective MSC-mediated-chondrogenesis. The *miR*-activated hydrogel shows a significant increase in key pro-chondrogenic articular cartilage genes without increasing hypertrophic differentiation, in addition to improved cartilage-like formation *in vitro*. Moreover, this advanced hydrogel system could be further evaluated for the delivery of various pro-chondrogenic nucleic acid therapeutics, as well as therapeutics targeting inflammatory pathways involved in OA. For instance, the interleukin-1 receptor antagonist (*IL-1Ra*), which has demonstrated potential in inhibiting OA-associated structural changes, could be delivered using this platform [50]. Furthermore, the hydrogel demonstrates significant potential for a wide range of applications beyond cartilage repair in tissue-specific regenerative medicine, providing a minimally invasive solution.

5. Conclusion

This study demonstrates that the incorporation of *miR-221* inhibitor delivered by GET-mediated transfection within a hydrogel designed specifically for cartilage repair is a promising approach for the treatment of cartilage damage. From a clinical perspective, the approach presented in this study, which has led to the development of a *miR-221* activated hydrogel, would be available as an injectable hydrogel for minimally invasive therapeutic delivery offering a promising new solution for the treatment of cartilage lesions and potentially early stage of OA. Furthermore, in terms of a wider application the technology developed in this project might be applicable to a broad range of tissue specific regenerative medicine applications by using different tissue specific gene therapeutics.

CRediT authorship contribution statement

Shan An: Writing – review & editing, Writing – original draft, Investigation, Conceptualization. **Claudio Intini:** Writing – review & editing, Writing – original draft, Investigation, Conceptualization. **Donagh O'Shea:** Conceptualization. **James E. Dixon:** Writing – review & editing. **Yiran Zheng:** Writing – review & editing. **Fergal J. O'Brien:** Writing – review & editing, Investigation, Funding acquisition, Conceptualization.

Declaration of competing interest

The authors declare that they have no known competing financial interests or personal relationships that could have appeared to influence the work reported in this paper.

Acknowledgements

This work was financially supported by the European Research Council (ERC) Advanced Grant n°788753 (ReCaP) and RCSI Soochow StAR International programme 2022.

Data availability

Data will be made available on request.

References

[1] P. Wang, S. Zhang, Q. Meng, P. Zhu, W. Yuan, Treatment and application of stem cells from different sources for cartilage injury: a literature review, Ann. Transl. Med. 10 (10) (2022) 610.
[2] G. Tavallaee, J.S. Rockel, S. Lively, M. Kapoor, MicroRNAs in synovial pathology associated with osteoarthritis, Front. Med. 7 (2020) 376.
[3] V.P. Leifer, J.N. Katz, E. Losina, The burden of OA-health services and economics, Osteoarthritis Cartilage 30 (1) (2022) 10–16.
[4] J. Martel-Pelletier, A.J. Barr, F.M. Cicuttini, P.G. Conaghan, C. Cooper, M. B. Goldring, S.R. Goldring, G. Jones, A.J. Teichtahl, J.P. Pelletier, Osteoarthritis, Nat. Rev. Dis. Prim. 2 (2016) 16072.
[5] J. Cibere, A. Thorne, J.A. Kopec, J. Singer, J. Canvin, D.B. Robinson, J. Pope, P. Hong, E. Grant, T. Lobanok, M. Ionescu, A.R. Poole, J.M. Esdaile, Glucosamine sulfate and cartilage type II collagen degradation in patients with knee osteoarthritis: randomized discontinuation trial results employing biomarkers, J. Rheumatol. 32 (5) (2005) 896–902.
[6] O. Korotkyi, A. Huet, K. Dvorshchenko, N. Kobyliak, T. Falalyeyeva, L. Ostapchenko, Probiotic composition and chondroitin sulfate regulate TLR-2/4-mediated NF-kappaB inflammatory pathway and cartilage metabolism in experimental osteoarthritis, Probiotics Antimicrob Proteins 13 (4) (2021) 1018–1032.
[7] M. Mihara, S. Higo, Y. Uchiyama, K. Tanabe, K. Saito, Different effects of high molecular weight sodium hyaluronate and NSAID on the progression of the cartilage degeneration in rabbit OA model, Osteoarthritis Cartilage 15 (5) (2007) 543–549.
[8] M.C.S. Inacio, E.W. Paxton, S.E. Graves, R.S. Namba, S. Nemes, Projected increase in total knee arthroplasty in the United States - an alternative projection model, Osteoarthritis Cartilage 25 (11) (2017) 1797–1803.
[9] C. Pabinger, H. Lothaller, A. Geissler, Utilization rates of knee-arthroplasty in OECD countries, Osteoarthritis Cartilage 23 (10) (2015) 1664–1673.
[10] C. Intini, T. Hodgkinson, S.M. Casey, J.P. Gleeson, F.J. O'Brien, Highly porous type II collagen-containing scaffolds for enhanced cartilage repair with reduced hypertrophic cartilage formation, Bioengineering (Basel) 9 (6) (2022).
[11] A. Perera, B. Lovrincevic, M. Pozar, Reply to the 'Comment on "Universal features in the lifetime distribution of clusters in hydrogen-bonding liquids"', Phys. Chem. Chem. Phys. 26 (6) (2024) 5717–5719, https://doi.org/10.1039/D3CP05269A. J. Grelska, Phys. Chem. Chem. Phys., 2024, 26.
[12] Y.Y. Liu, C. Intini, M. Dobricic, F.J. O'Brien, L.L. J, M. Echeverry-Rendon, Collagen-based 3D printed poly (glycerol sebacate) composite scaffold with biomimicking mechanical properties for enhanced cartilage defect repair, Int. J. Biol. Macromol. 280 (Pt 2) (2024) 135827.
[13] R.M. Raftery, A.G. Gonzalez Vazquez, G. Chen, F.J. O'Brien, Activation of the SOX-5, SOX-6, and SOX-9 Trio of transcription factors using a gene-activated scaffold stimulates mesenchymal stromal cell chondrogenesis and inhibits endochondral ossification, Adv. Healthcare Mater. 9 (10) (2020) e1901827.
[14] A.L. Laiva, R.M. Raftery, M.B. Keogh, F.J. O'Brien, Pro-angiogenic impact of SDF-1alpha gene-activated collagen-based scaffolds in stem cell driven angiogenesis, Int. J. Pharm. 544 (2) (2018) 372–379.
[15] E. Andres Sastre, Y. Nossin, I. Jansen, N. Kops, C. Intini, J. Witte-Bouma, B. van Rietbergen, S. Hofmann, Y. Ridwan, J.P. Gleeson, F.J. O'Brien, E.B. Wolvius, G. van Osch, E. Farrell, A new semi-orthotopic bone defect model for cell and biomaterial testing in regenerative medicine, Biomaterials 279 (2021) 121187.
[16] C. Intini, M. Lemoine, T. Hodgkinson, S. Casey, J.P. Gleeson, F.J. O'Brien, A highly porous type II collagen containing scaffold for the treatment of cartilage defects enhances MSC chondrogenesis and early cartilaginous matrix deposition, Biomater. Sci. 10 (4) (2022) 970–983.
[17] T. Gonzalez-Fernandez, E.G. Tierney, G.M. Cunniffe, F.J. O'Brien, D.J. Kelly, Gene delivery of TGF-beta3 and BMP2 in an MSC-laden alginate hydrogel for articular cartilage and endochondral bone tissue engineering, Tissue Eng. 22 (9–10) (2016) 776–787.
[18] Q. Chai, Y. Jiao, X. Yu, Hydrogels for biomedical applications: their characteristics and the mechanisms behind them, Gels 3 (1) (2017).
[19] F. Picard, A. Deakin, N. Balasubramanian, A. Gregori, Minimally invasive total knee replacement: techniques and results, Eur. J. Orthop. Surg. Traumatol. 28 (5) (2018) 781–791.
[20] A.J. Sophia Fox, A. Bedi, S.A. Rodeo, The basic science of articular cartilage: structure, composition, and function, Sport Health 1 (6) (2009) 461–468.
[21] K.L. Spiller, S.A. Maher, A.M. Lowman, Hydrogels for the repair of articular cartilage defects, Tissue Eng., Part B 17 (4) (2011) 281–299.
[22] D.G. O'Shea, T. Hodgkinson, C.M. Curtin, F.J. O'Brien, An injectable and 3D printable pro-chondrogenic hyaluronic acid and collagen type II composite hydrogel for the repair of articular cartilage defects, Biofabrication 16 (1) (2023).
[23] M.T. Poldervaart, B. Goversen, M. de Ruijter, A. Abbadessa, F.P.W. Melchels, F. C. Oner, W.J.A. Dhert, T. Vermonden, J. Alblas, 3D bioprinting of methacrylated hyaluronic acid (MeHA) hydrogel with intrinsic osteogenicity, PLoS One 12 (6) (2017) e0177628.
[24] M. Wang, Z. Deng, Y. Guo, P. Xu, Designing functional hyaluronic acid-based hydrogels for cartilage tissue engineering, Mater Today Bio 17 (2022) 100495.
[25] K. Chen, N. Rajewsky, The evolution of gene regulation by transcription factors and microRNAs, Nat. Rev. Genet. 8 (2) (2007) 93–103.
[26] N.Z. Laird, T.M. Acri, K. Tingle, A.K. Salem, Gene- and RNAi-activated scaffolds for bone tissue engineering: current progress and future directions, Adv. Drug Deliv. Rev. 174 (2021) 613–627.
[27] E.G. Tierney, G.P. Duffy, S.A. Cryan, C.M. Curtin, F.J. O'Brien, Non-viral gene-activated matrices: next generation constructs for bone repair, Organogenesis 9 (1) (2013) 22–28.
[28] I. Mencia Castano, C.M. Curtin, G.P. Duffy, F.J. O'Brien, Next generation bone tissue engineering: non-viral miR-133a inhibition using collagen-nanohydroxyapatite scaffolds rapidly enhances osteogenesis, Sci. Rep. 6 (2016) 27941.

[29] R.M. Raftery, I. Mencia Castano, G. Chen, B. Cavanagh, B. Quinn, C.M. Curtin, S. A. Cryan, F.J. O'Brien, Translating the role of osteogenic-angiogenic coupling in bone formation: highly efficient chitosan-pDNA activated scaffolds can accelerate bone regeneration in critical-sized bone defects, Biomaterials 149 (2017) 116–127.
[30] E.G. Tierney, K. McSorley, C.L. Hastings, S.A. Cryan, T. O'Brien, M.J. Murphy, F. P. Barry, F.J. O'Brien, G.P. Duffy, High levels of ephrinB2 over-expression increases the osteogenic differentiation of human mesenchymal stem cells and promotes enhanced cell mediated mineralisation in a polyethyleneimine-ephrinB2 gene-activated matrix, J. Contr. Release 165 (3) (2013) 173–182.
[31] F.J. O'Brien, D.J. Kelly, J.E. Dixon, C. Intini, T. Hodgkinson, M. Joyce, Gene activated reinforced scaffolds for SOX9 delivery to enhance repair of large load bearing articular cartilage defects, Eur. Cell. Mater. 47 (2024) 91–108.
[32] D. Kim, J. Song, E.J. Jin, MicroRNA-221 regulates chondrogenic differentiation through promoting proteosomal degradation of slug by targeting Mdm2, J. Biol. Chem. 285 (35) (2010) 26900–26907.
[33] A. Lolli, E. Lambertini, L. Penolazzi, M. Angelozzi, C. Morganti, T. Franceschetti, S. Pelucchi, R. Gambari, R. Piva, Pro-chondrogenic effect of miR-221 and slug depletion in human MSCs, Stem Cell Rev Rep 10 (6) (2014) 841–855.
[34] A. Lolli, R. Narcisi, E. Lambertini, L. Penolazzi, M. Angelozzi, N. Kops, S. Gasparini, G.J. van Osch, R. Piva, Silencing of antichondrogenic MicroRNA-221 in human mesenchymal stem cells promotes cartilage repair in vivo, Stem Cell. 34 (7) (2016) 1801–1811.
[35] C. Intini, L.B. Ferreras, S. Casey, J.E. Dixon, J.P. Gleeson, F.J. O'Brien, An innovative miR-activated scaffold for the delivery of a miR-221 inhibitor to enhance cartilage defect repair, Advanced Therapeutics 6 (7) (2023).
[36] J.E. Dixon, V. Wellington, A. Elnima, H.M. Eltaher, Effects of microenvironment and dosing on efficiency of enhanced cell penetrating peptide nonviral gene delivery, ACS Omega 9 (4) (2024) 5014–5023.
[37] S. Rehmani, C.M. McLaughlin, H.M. Eltaher, R.C. Moffett, P.R. Flatt, J.E. Dixon, Orally-delivered insulin-peptide nanocomplexes enhance transcytosis from cellular depots and improve diabetic blood glucose control, J. Contr. Release 360 (2023) 93–109.
[38] R.B. So, G. Li, V. Brentville, J.M. Daly, J.E. Dixon, Combined biolistic and cell penetrating peptide delivery for the development of scalable intradermal DNA vaccines, J. Contr. Release 367 (2024) 209–222.
[39] R.N. Power, B.L. Cavanagh, J.E. Dixon, C.M. Curtin, F.J. O'Brien, Development of a gene-activated scaffold incorporating multifunctional cell-penetrating peptides for pSDF-1alpha delivery for enhanced angiogenesis in tissue engineering applications, Int. J. Mol. Sci. 23 (3) (2022).
[40] M. Joyce, T. Hodgkinson, M. Lemoine, A. González-Vázquez, D.J. Kelly, F. J. O'Brien, Development of a 3D-printed bioabsorbable composite scaffold with mechanical properties suitable for treating large, load-bearingarticular cartilage defects, Eur. Cell. Mater. 45 (2023) 158–172.
[41] A. Lolli, K. Sivasubramaniyan, M.L. Vainieri, J. Oieni, N. Kops, A. Yayon, G. van Osch, Hydrogel-based delivery of antimiR-221 enhances cartilage regeneration by endogenous cells, J. Contr. Release 309 (2019) 220–230.
[42] C. Antich, J. de Vicente, G. Jimenez, C. Chocarro, E. Carrillo, E. Montanez, P. Galvez-Martin, J.A. Marchal, Bio-inspired hydrogel composed of hyaluronic acid and alginate as a potential bioink for 3D bioprinting of articular cartilage engineering constructs, Acta Biomater. 106 (2020) 114–123.
[43] I. Noh, N. Kim, H.N. Tran, J. Lee, C. Lee, 3D printable hyaluronic acid-based hydrogel for its potential application as a bioink in tissue engineering, Biomater. Res. 23 (2019) 3.
[44] J. Liang, P. Liu, X. Yang, L. Liu, Y. Zhang, Q. Wang, H. Zhao, Biomaterial-based scaffolds in promotion of cartilage regeneration: recent advances and emerging applications, J Orthop Translat 41 (2023) 54–62.
[45] M. Merola, S. Affatato, Materials for hip prostheses: a review of wear and loading considerations, Materials 12 (3) (2019).
[46] K.D. Ngadimin, A. Stokes, P. Gentile, A.M. Ferreira, Biomimetic hydrogels designed for cartilage tissue engineering, Biomater. Sci. 9 (12) (2021) 4246–4259.
[47] B. Cao, Z. Li, R. Peng, J. Ding, Effects of cell-cell contact and oxygen tension on chondrogenic differentiation of stem cells, Biomaterials 64 (2015) 21–32.
[48] H. Thorp, K. Kim, S. Bou-Ghannam, M. Kondo, T. Maak, D.W. Grainger, T. Okano, Enhancing chondrogenic potential via mesenchymal stem cell sheet multilayering, Regen Ther 18 (2021) 487–496.
[49] M.T. Manley, D.M. Gaisser, M. Uratsuji, B.N. Stulberg, T.W. Bauer, L.S. Stern, Fixation of porous titanium and smooth hydroxylapatite interfaces in a loaded model, 34th Annual Meeting ORS, Feb. 1-4, Atlanta 13 (1988) 332.
[50] W.A. Lackington, M.A. Gomez-Sierra, A. Gonzalez-Vazquez, F.J. O'Brien, M. J. Stoddart, K. Thompson, Non-viral gene delivery of interleukin-1 receptor antagonist using collagen-hydroxyapatite scaffold protects rat BM-MSCs from IL-1beta-mediated inhibition of osteogenesis, Front. Bioeng. Biotechnol. 8 (2020) 582012.